

Universal Spectral Tokenization via Self-Supervised Panchromatic Representation Learning

Jeff Shen^{*,1}, Francois Lanusse^{2,3}, Liam Parker^{6,3,4,5}, Ollie Liu⁷, Tom Hehir⁸
 Leopoldo Sarra³, Lucas Meyer³, Micah Bowles⁹, Sebastian Wagner-Carena^{3,5}
 Helen Qu³, Siavash Golkar^{3,5}, Alberto Bietti³, Hatim Bourfoune¹⁰, Nathan Cassereau¹⁰
 Pierre Cornette¹⁰, Keiya Hirashima^{3,11}, Geraud Krawezik³, Ruben Ohana³, Nicholas Lourie⁵
 Michael McCabe^{3,5}, Rudy Morel³, Payel Mukhopadhyay^{1,8}, Mariel Pettee¹²
 Bruno Regaldo-Saint Blancard³, KyungHyun Cho⁵, Miles Cranmer⁸, Shirley Ho^{1,3,5}

The Polymathic AI Collaboration

¹Princeton University, ²Université Paris-Saclay, Université Paris Cité, CEA, CNRS, AIM, ³Flatiron Institute, ⁴Lawrence Berkeley National Laboratory, ⁵New York University, ⁶University of California, Berkeley, ⁷University of Southern California, ⁸University of Cambridge, ⁹University of Oxford, ¹⁰IDRIS, CNRS, ¹¹RIKEN Center for iTHEMS, ¹²University of Wisconsin–Madison

Abstract

Sequential scientific data span many resolutions and domains, and unifying them into a common representation is a key step toward developing foundation models for the sciences. Astronomical spectra exemplify this challenge: massive surveys have collected millions of spectra across a wide range of wavelengths and resolutions, yet analyses remain fragmented across spectral domains (e.g., optical vs. infrared) and object types (e.g., stars vs. galaxies), limiting the ability to pool information across datasets. We present a deep learning model that jointly learns from heterogeneous spectra in a self-supervised manner. Our universal spectral tokenizer processes spectra from a variety of object types and resolutions directly on their native wavelength grids, producing intrinsically aligned, homogeneous, and physically meaningful representations that can be efficiently adapted to achieve competitive performance across a range of downstream tasks. For the first time, we demonstrate that a single model can unify spectral data across resolutions and domains, suggesting that our model can serve as a powerful building block for foundation models in astronomy—and potentially extend to other scientific domains with heterogeneous sequential data, such as climate and healthcare.

1 Introduction

Spectra encode fundamental astrophysical information, from stellar chemical abundances to galaxy dynamics and the state of the intergalactic medium. Large-scale surveys such as SDSS, DESI, GALAH, and APOGEE [Abdurro'uf et al., 2022; Buder et al., 2021; DESI Collaboration et al., 2025] have collected millions of spectra across a wide range of wavelengths ($R \sim 2,000\text{--}28,000$) and science targets. However, analysis pipelines remain fragmented: each survey typically requires bespoke preprocessing and task-specific machine learning (ML) models. This siloed approach limits flexibility, prevents the reuse of knowledge across datasets, and makes it impossible to combine heterogeneous information into a shared representation. Moreover, training a new model for every instrument, object class, or task is inefficient, hinders generalization, and stands in contrast to the foundation model paradigm that is beginning to take hold in astronomy [e.g., Parker et al., 2024;

*shenjeff@princeton.edu

Rizhko and Bloom, 2024; Smith et al., 2024]. Beyond astronomy, this challenge reflects a broader problem: how to learn universal representations from irregular, multiresolution sequential data—a setting that also arises in time series across physics, climate, and healthcare.

We propose a universal tokenizer for spectra that directly ingests native wavelength grids without resampling, enabling seamless integration across surveys. Because the architecture is resolution- and domain-agnostic, the same design naturally extends beyond spectra; for example, wavelength embeddings can be swapped for time-based embeddings to tokenize irregular, multiresolution time series. This positions our approach as a flexible building block for scientific foundation models, in astronomy and more broadly.

Related work Physically motivated spectral models fit forward models to spectra, offering interpretability but suffering from model misspecification and poor scalability. On the data-driven side, supervised approaches achieve high accuracy where labels exist, but are survey-specific and limited by label availability. Koblischke and Bovy [2024] show, using a similar encoder to the one we propose, that a foundation model approach (pretraining, then fine-tuning) can reduce the limitations of label availability on a stellar parameter regression problem using APOGEE spectra. Self-supervised spectral models [e.g., Melchior et al., 2022; Portillo et al., 2020] have been explored in single domains on fixed (latent) grids, which introduce interpolation artifacts and scale poorly across wide wavelength ranges. Furthermore, they typically require a good estimate of the redshift before processing.² In contrast, our approach requires nothing but the spectrum. Contrastive methods [Buck and Schwarz, 2024; Zhao et al., 2025] learn spectral representations but still rely on survey-specific encoders/decoders. In contrast, our approach scales to arbitrary datasets with a single encoder and decoder.

Contributions To our knowledge, no prior work has demonstrated a single model that can pretrain jointly across heterogeneous spectroscopic surveys (optical and IR; low- and high-resolution; stars, galaxies, and quasars) on their native wavelength grids without homogenization, while also providing an architecture that naturally extends to other forms of irregular, multiresolution sequential data such as time series. Our contributions are: (1) a novel architecture that directly ingests sequential data on arbitrary combinations of wavelength/time grids, (2) a panchromatic, multi-resolution, self-supervised pretraining strategy applied to SDSS, DESI, GALAH, and APOGEE, yielding cross-domain, homogeneous, and rich representations under a single model, and (3) demonstration that lightweight adaptation of these embeddings achieves competitive performance on downstream tasks such as object classification and stellar parameter regression relative to task-specific baselines.

2 A Universal Spectrum Tokenizer

Our model is based on a Vision Transformer (ViT) architecture [Dosovitskiy et al., 2021], adapted for one-dimensional spectral data. In particular, our innovative encoder creates homogeneous, wavelength-aware embeddings from heterogeneous input spectra, allowing these embeddings to be used for a variety of downstream tasks. Furthermore, the architecture allows the model to be easily extended to pretraining with a masked autoencoding or contrastive objective. A diagram of the overall architecture and pretraining process is shown in Figure 1.

Input processing and encoding Each spectrum provides flux values with measurement errors, per-pixel wavelengths, and a mask for problematic pixels. We normalize spectra by dividing out the median flux, ensuring the model focuses on relative variations. The normalized flux and error values are then segmented into fixed-size patches, projected into a high-dimensional embedding space. We also construct a patch-level mask that excludes patches dominated by bad or padded pixels (e.g., due to detector failures): if at least half of the pixels within a patch are bad, we mark the patch as bad.

To handle non-uniform wavelength grids, we add continuous per-pixel sinusoidal embeddings [Rózański et al., 2023], avoiding the interpolation errors and inefficiencies of fixed latent grids [e.g., Melchior et al., 2022]. For wavelength λ and frequency scale ω_k , the embedding is

$$\text{PE}(\lambda)_k = \begin{cases} \sin(\omega_k \lambda), & k \text{ even}, \\ \cos(\omega_k \lambda), & k \text{ odd}, \end{cases} \quad \omega_k \in \left[\frac{2\pi}{\max_period}, \frac{2\pi}{\min_period} \right], \quad (1)$$

with $\{\omega_k\}$ log-spaced between $\frac{2\pi}{\max_period}$ and $\frac{2\pi}{\min_period}$. Wavelength embeddings are patched and added to the flux patches, imbuing the tokens with wavelength information. These representations are

²This can be problematic as obtaining a good estimate of the redshift requires a good spectral model, thus leading to a chicken-and-egg problem.

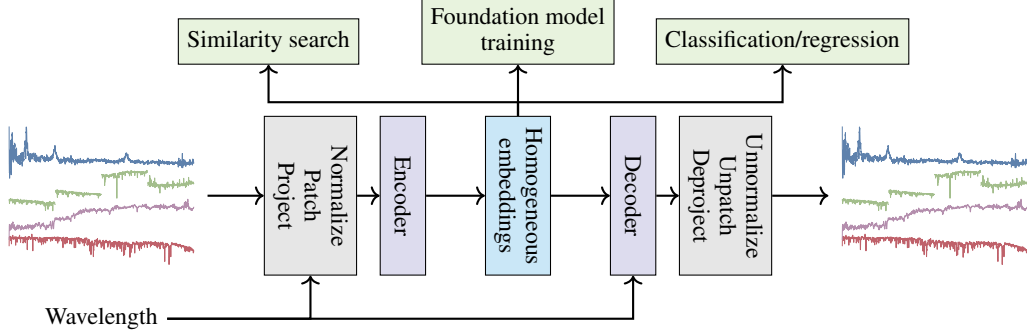


Figure 1: Overview of the universal spectrum tokenizer. The encoder creates homogeneous, wavelength-aware embeddings from heterogeneous input spectra; these can be used for a variety of downstream tasks. The decoder reconstructs the input spectrum from the learned representations.

Table 1: Summary of spectroscopic datasets used for training.

Dataset	Wavelength Range	Resolution	Objects
SDSS DR17 [Abdurro’uf et al., 2022]	3600–10400 Å	$R \sim 2000$	galaxies, quasars, stars
DESI DR1 [DESI Collaboration et al., 2025]	3600–9800 Å	$R \sim 5000$	galaxies, quasars, stars
GALAH DR3 [Buder et al. [2021]]	4700–7900 Å	$R \sim 28,000$	stars
APOGEE [Abdurro’uf et al., 2022]	1.51–1.7 μm	$R \sim 22,500$	stars

processed by a series of transformer blocks [Vaswani et al., 2017], which consist of alternating multi-head self-attention and feed-forward layers. Crucially, the attention mechanism allows the model to learn long-range dependencies between different parts of the spectrum, such as correlated line features that span large wavelength ranges. This is particularly important for spectral data, where features can span large wavelength ranges and may not be immediately adjacent in the input sequence. Bad patches are ignored in the attention computation according to the patch mask. The output is, for each spectrum, a sequence of tokens with a sequence dimension (with length equal to the original sequence length divided by the patch size) and a small channel dimension, representing wavelength-aware spectral features; these can be used for various downstream tasks such as classification, regression, or reconstruction.

Decoding and reconstruction For self-supervised pretraining, we use a loss-aware reconstruction objective, which encourages the model to reconstruct the original input spectrum from the learned representations. The decoder mirrors the encoder; the decoding process proceeds by first requesting an output wavelength grid, and adding its sinusoidal embedding to the encoder tokens to provide the model with information about where we want to reconstruct the signal. The decoder then processes the tokens to produce a sequence of outputs, which are unpatched to produce a per-pixel reconstruction of the input spectrum. The reconstruction loss is a Gaussian likelihood between the reconstructed spectrum and the original input spectrum and is only computed for valid pixels: $\mathcal{L} = \frac{1}{N} \sum_{i=1}^N m_i \frac{(y_i - \hat{y}_i)^2}{\sigma_i^2}$, where N is the number of valid pixels, and m_i , y_i , \hat{y}_i , and σ_i are the validity mask, original flux, reconstructed flux, and measurement error at pixel i .

Dataset We train our model using spectroscopic data from four major surveys: SDSS DR17, GALAH DR3, DESI DR1, and APOGEE; the data are accessed through the Multimodal Universe [The Multimodal Universe Collaboration et al., 2024] project. We provide details about the datasets in Table 1; we emphasize that our model is trained across all of these datasets without homogenization, efficiently leveraging the native wavelength grids and resolutions of each survey. Doing the same with a fixed grid model such as the one in Melchior et al. [2022] would require a grid size of 300K pixels—an impossibility.

Training and implementation details We use 6 encoder and 6 decoder transformer blocks, an embedding dimension of 512, 8 attention heads, and a patch size of 32 pixels. We use a batch size of 64, a constant learning rate of 1e-4, and the AdamW optimizer [Loshchilov and Hutter, 2019] with $\beta_1 = 0.9$, $\beta_2 = 0.999$, and weight decay of 0.01. We train for 600k steps on 4 NVIDIA A100-SXM4-40GB GPUs, which takes 48 hours.

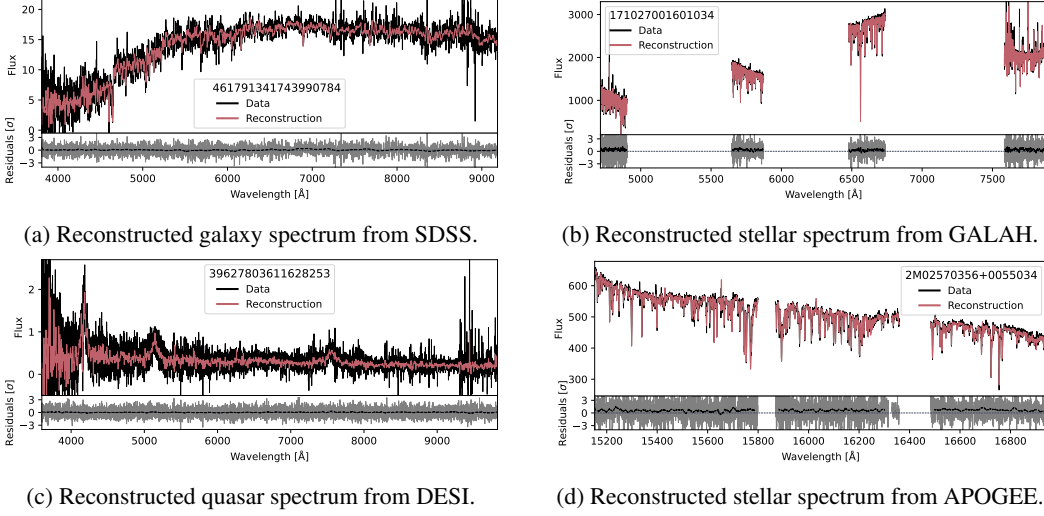


Figure 2: Examples of reconstructed spectra from the model for three different object types and four different surveys. Each subplot represents a different dataset. The top panels show the original spectrum in black and the reconstructed spectrum in red. The bottom panels show the residuals, with raw values in grey and a smoothed version in black. Figures are best viewed zoomed in.

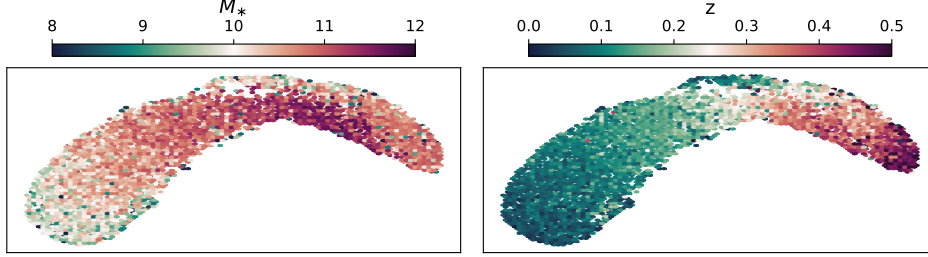


Figure 3: UMAP visualization of mean-pooled embeddings for 10,000 SDSS galaxies. The x and y axes are arbitrary. The panels are coloured by stellar mass (**left**) and redshift (**right**), and show that the embeddings have strong correlations with these physical properties.

3 Results

This section shows that our model adapts to diverse tasks with minimal training, capturing information across spectral domains and object types. Our aim here is not to achieve state-of-the-art performance, but to demonstrate broad applicability. We leave multi-modal and cross-survey tasks to future foundation models built on top of our universal tokenizer, while emphasizing that, unlike task-specific pipelines, our model is reusable across many settings.

Spectrum reconstruction We show examples of autoencoded spectra for each of our four datasets in Figure 2. These datasets span multiple orders of magnitude in flux and exhibit a wide variety of physical phenomena and spectral features, yet a single model with our design is able to reconstruct them all. Because the tokenizer operates directly on native wavelength grids, it naturally captures information across multiple scales—ranging from broad continuum shapes to narrow absorption and emission lines—without requiring any dataset-specific preprocessing.

Structure of the latent space Following Melchior et al. [2022], we use UMAP to examine the structure of the learned embedding space in Figure 3. Here we perform this visualization for 10,000 randomly selected SDSS galaxies with no redshift warnings or plate quality issues. We then apply UMAP to the mean-pooled embeddings³ to reduce the dimensionality to 2D for visualization. When we color the points by either their stellar mass, which is obtained from the FIREFLY spectral fitting

³This collapses the wavelength-dependent information in the embeddings, with expected loss of intra-spectrum details; however, this is sufficient for our goal of performing a qualitative analysis of the overall structure of the embedding space.

code with the ELODIE library [Comparat et al., 2019; Prugniel and Soubiran, 2001], or by redshift, we see clear color gradients in the embedding space, indicating that the embeddings are highly correlated with these physical properties. We again emphasize that the upstream ViT model that produced these embeddings was trained without any notion of downstream “derived” labels; the only data it has seen are raw spectra, and the visible structure is emergent.

Object classification We evaluate our model on the task of object classification, where the goal is to classify spectra into different object types (galaxies, stars, quasars). We train a lightweight adaptation module on top of the embeddings from our (frozen) pretrained universal spectrum tokenizer. In Table 2 we show that this achieves competitive performance in comparison to a strong task-specific baseline from Zhong et al. [2024]. We note that our adaptation module is generic with respect to the data and task; in fact, we use the exact same architecture for the physical parameter estimation task below. Furthermore, because the embeddings from our universal tokenizer are already informative, this adaptation module is extremely lightweight and capable of achieving strong performance with only a fraction of the training time as compared to a from-scratch model.

Physical parameter estimation We train an adaptation module on top of our pretrained universal spectrum tokenizer to regress physical parameters—effective temperature (T_{eff}), surface gravity ($\log g$), and metallicity ([Fe/H])—from APOGEE stellar spectra. We use ASPCAP estimates [García Pérez et al., 2016] as the ground truth labels for training and evaluation; typical uncertainties from the pipeline are $\sigma_{T_{\text{eff}}} = 2\%$ (~ 100 K for a 5000 K star), $\sigma_{\log g} = 0.1$ dex, and $\sigma_{[\text{Fe}/\text{H}]} = 0.05$ dex⁴. Following Leung and Bovy [2018], we report performance as scaled median absolute deviation $\sigma_{\text{MAD}} \approx 1.4826$ MAD, a robust measure of dispersion. We show in Table 3 that the performance of an adaptation module on top of our tokenizer is competitive against several well-known strong baselines, and well within uncertainties of the ASPCAP pipeline.

Table 2: Performance on object classification from DESI spectra. The results are reported as accuracy (percentage of correctly classified objects). **Higher is better.**

Model	Galaxy	QSO	Star	Average
Zhong et al. [2024]	93%	99%	98%	96%
Ours w/ adaptation	94%	97%	98%	96%

Table 3: Performance on stellar parameter estimation from APOGEE spectra. * indicates errors expressed as σ of residuals, and † indicates σ_{MAD} of residuals, in the respective units. **Lower is better.**

Model	$\log g$	T_{eff}	[Fe/H]
Casey et al. [2016]*	0.07 dex	38 K	0.03 dex
Leung and Bovy [2018] [†]	0.05 dex	30 K	0.02 dex
Olney et al. [2020]*	0.15 dex	100 K	0.07 dex
Ours w/ adaptation [†]	0.07 dex	23 K	0.02 dex

4 Conclusion

We have introduced the first universal spectral tokenizer capable of learning aligned representations across heterogeneous astronomical surveys without resampling or homogenization. The model produces physically meaningful embeddings that can be efficiently adapted to diverse downstream tasks, achieving competitive performance with task-specific baselines. Beyond enabling cross-survey analyses and knowledge transfer between previously isolated spectral domains, our approach provides a general framework for unifying highly heterogeneous sequential data, such time series, in a domain-agnostic and scalable fashion.

Acknowledgments and Disclosure of Funding

The authors would like to acknowledge the Center for Computational Astrophysics at the Flatiron Institute for hospitality while a portion of this work was carried out. In addition, the data used in this work are hosted on equipment supported by the Scientific Computing Core at the Flatiron Institute, a division of the Simons Foundation. JS is supported by the Natural Sciences and Engineering Research Council of Canada (NSERC), funding reference number 587652, and by the Citadel GQS PhD Fellowship in Physics. Polymathic AI and SH gratefully acknowledge the support provided by Schmidt Sciences and Simons Foundation.

⁴dex is used to denote an order of magnitude. Two numbers that differ by a factor of 10 differ by 1 dex, those that differ by a factor of 100 differ by 2 dex, and so on.

Funding for the Sloan Digital Sky Survey IV has been provided by the Alfred P. Sloan Foundation, the U.S. Department of Energy Office of Science, and the Participating Institutions.

SDSS-IV acknowledges support and resources from the Center for High Performance Computing at the University of Utah. The SDSS website is www.sdss4.org.

SDSS-IV is managed by the Astrophysical Research Consortium for the Participating Institutions of the SDSS Collaboration including the Brazilian Participation Group, the Carnegie Institution for Science, Carnegie Mellon University, Center for Astrophysics | Harvard & Smithsonian, the Chilean Participation Group, the French Participation Group, Instituto de Astrofísica de Canarias, The Johns Hopkins University, Kavli Institute for the Physics and Mathematics of the Universe (IPMU) / University of Tokyo, the Korean Participation Group, Lawrence Berkeley National Laboratory, Leibniz Institut für Astrophysik Potsdam (AIP), Max-Planck-Institut für Astronomie (MPIA Heidelberg), Max-Planck-Institut für Astrophysik (MPA Garching), Max-Planck-Institut für Extraterrestrische Physik (MPE), National Astronomical Observatories of China, New Mexico State University, New York University, University of Notre Dame, Observatório Nacional / MCTI, The Ohio State University, Pennsylvania State University, Shanghai Astronomical Observatory, United Kingdom Participation Group, Universidad Nacional Autónoma de México, University of Arizona, University of Colorado Boulder, University of Oxford, University of Portsmouth, University of Utah, University of Virginia, University of Washington, University of Wisconsin, Vanderbilt University, and Yale University.

This research used data obtained with the Dark Energy Spectroscopic Instrument (DESI). DESI construction and operations is managed by the Lawrence Berkeley National Laboratory. This material is based upon work supported by the U.S. Department of Energy, Office of Science, Office of High-Energy Physics, under Contract No. DE-AC02-05CH11231, and by the National Energy Research Scientific Computing Center, a DOE Office of Science User Facility under the same contract. Additional support for DESI was provided by the U.S. National Science Foundation (NSF), Division of Astronomical Sciences under Contract No. AST-0950945 to the NSF's National Optical-Infrared Astronomy Research Laboratory; the Science and Technology Facilities Council of the United Kingdom; the Gordon and Betty Moore Foundation; the Heising-Simons Foundation; the French Alternative Energies and Atomic Energy Commission (CEA); the National Council of Humanities, Science and Technology of Mexico (CONAHCYT); the Ministry of Science and Innovation of Spain (MICINN), and by the DESI Member Institutions: www.desi.lbl.gov/collaborating-institutions. The DESI collaboration is honored to be permitted to conduct scientific research on I'oligam Du'ag (Kitt Peak), a mountain with particular significance to the Tohono O'odham Nation. Any opinions, findings, and conclusions or recommendations expressed in this material are those of the author(s) and do not necessarily reflect the views of the U.S. National Science Foundation, the U.S. Department of Energy, or any of the listed funding agencies.

This work made use of the Third Data Release of the GALAH Survey (Buder et al. 2021). The GALAH Survey is based on data acquired through the Australian Astronomical Observatory, under programs: A/2013B/13 (The GALAH pilot survey); A/2014A/25, A/2015A/19, A/2017A/18 (The GALAH survey phase 1); A/2018A/18 (Open clusters with HERMES); A/2019A/1 (Hierarchical star formation in Ori OB1); A/2019A/15 (The GALAH survey phase 2); A/2015B/19, A/2016A/22, A/2016B/10, A/2017B/16, A/2018B/15 (The HERMES-TESS program); and A/2015A/3, A/2015B/1, A/2015B/19, A/2016A/22, A/2016B/12, A/2017A/14 (The HERMES K2-follow-up program). We acknowledge the traditional owners of the land on which the AAT stands, the Gamilaraay people, and pay our respects to elders past and present. This paper includes data that has been provided by AAO Data Central (datacentral.org.au).

References

- Abdurro'uf, Katherine Accetta, Conny Aerts, Víctor Silva Aguirre, Romina Ahumada, Nikhil Ajgaonkar, N. Filiz Ak, Shadab Alam, Carlos Allende Prieto, Andrés Almeida, Friedrich Anders, Scott F. Anderson, Brett H. Andrews, Borja Anguiano, Erik Aquino-Ortíz, Alfonso Aragón-Salamanca, María Argudo-Fernández, Metin Ata, Marie Aubert, Vladimir Avila-Reese, Carles Badenes, Rodolfo H. Barbá, Kat Barger, Jorge K. Barrera-Ballesteros, Rachael L. Beaton, Timothy C. Beers, Francesco Belfiore, Chad F. Bender, Mariangela Bernardi, Matthew A. Bershadsky, Florian Beutler, Christian Moni Bidin, Jonathan C. Bird, Dmitry Bizyaev, Guillermo A. Blanc, Michael R. Blanton, Nicholas Fraser Boardman, Adam S. Bolton, Médéric Boquien, Jura Borissova, Jo Bovy, W. N. Brandt, Jordan Brown, Joel R. Brownstein, Marcella Brusa, Johannes Buchner, Kevin Bundy, Joseph N. Burchett, Martin Bureau, Adam Burgasser, Tuesday K. Cabang, Stephanie Campbell, Michele Cappellari, Joleen K. Carlberg, Fábio Carneiro Wanderley, Ricardo Carrera,

Jennifer Cash, Yan-Ping Chen, Wei-Huai Chen, Brian Cherinka, Cristina Chiappini, Peter Doohyun Choi, S. Drew Chojnowski, Haeun Chung, Nicolas Clerc, Roger E. Cohen, Julia M. Comerford, Johan Comparat, Luiz da Costa, Kevin Covey, Jeffrey D. Crane, Irene Cruz-Gonzalez, Connor Culhane, Katia Cunha, Y. Sophia 昱Dai 戴, Guillermo Damke, Jeremy Darling, James W. Davidson Jr., Roger Davies, Kyle Dawson, Nathan De Lee, Aleksandar M. Diamond-Stanic, Mariana Cano-Díaz, Helena Domínguez Sánchez, John Donor, Chris Duckworth, Tom Dwelly, Daniel J. Eisenstein, Yvonne P. Elsworth, Eric Emsellem, Mike Eracleous, Stephanie Escoffier, Xiaohui Fan, Emily Farr, Shuai Feng, José G. Fernández-Trincado, Diane Feuillet, Andreas Filipp, Sean P Fillingham, Peter M. Frinchaboy, Sébastien Fromenteau, Lluís Galbany, Rafael A. García, D. A. García-Hernández, Junqiang Ge, Doug Geisler, Joseph Gelfand, Tobias Géron, Benjamin J. Gibson, Julian Goddy, Diego Godoy-Rivera, Kathleen Grabowski, Paul J. Green, Michael Greener, Catherine J. Grier, Emily Griffith, Hong Guo, Julien Guy, Massinissa Hadjara, Paul Harding, Sten Hasselquist, Christian R. Hayes, Fred Hearty, Jesús Hernández, Lewis Hill, David W. Hogg, Jon A. Holtzman, Danny Horta, Bau-Ching Hsieh, Chin-Hao Hsu, Yun-Hsin Hsu, Daniel Huber, Marc Huertas-Company, Brian Hutchinson, Ho Seong Hwang, Héctor J. Ibarra-Medel, Jacob Ider Chitham, Gabriele S. Ilha, Julie Imig, Will Jaekle, Tharindu Jayasinghe, Xihan Ji, Jennifer A. Johnson, Amy Jones, Henrik Jónsson, Ivan Katkov, Dr. Arman Khalatyan, Karen Kinemuchi, Shobhit Kisku, Johan H. Knapen, Jean-Paul Kneib, Juna A. Kollmeier, Miranda Kong, Marina Kounkel, Kathryn Kreckel, Dhanes Krishnarao, Ivan Lacerna, Richard R. Lane, Rachel Langgin, Ramon Lavender, David R. Law, Daniel Lazarz, Henry W. Leung, Ho-Hin Leung, Hannah M. Lewis, Cheng Li, Ran Li, Jianhui Lian, Fu-Heng Liang, Lihwai 林 Lin, Yen-Ting Lin, Sicheng Lin, Chris Lintott, Dan Long, Penélope Longa-Peña, Carlos López-Cobá, Shengdong Lu, Britt F. Lundgren, Yuanze Luo, J. Ted Mackereth, Axel de la Macorra, Suvrath Mahadevan, Steven R. Majewski, Arturo Manchado, Travis Mandeville, Claudia Maraston, Berta Margalef-Bentabol, Thomas Masseron, Karen L. Masters, Savita Mathur, Richard M. McDermid, Myles McKay, Andrea Merloni, Michael Merrifield, Szabolcs Meszaros, Andrea Miglio, Francesco Di Mille, Dante Minniti, Rebecca Minsley, Antonela Monachesi, Jeongin Moon, Benoit Mosser, John Mulchaey, Demitri Muna, Ricardo R. Muñoz, Adam D. Myers, Natalie Myers, Seshadri Nadathur, Preethi Nair, Kirpal Nandra, Justus Neumann, Jeffrey A. Newman, David L. Nidever, Farnik Nikakhtar, Christian Nitschelm, Julia E. O'Connell, Luis Garma-Oehmichen, Gabriel Luan Souza de Oliveira, Richard Olney, Daniel Oravetz, Mario Ortigoza-Urdaneta, Yeisson Osorio, Justin Otter, Zachary J. Pace, Nelson Padilla, Kaike Pan, Hsi-An Pan, Tanya Parikh, James Parker, Sébastien Peirani, Karla Peña Ramírez, Samantha Penny, Will J. Percival, Ismael Perez-Fournon, Marc Pinsonneault, Frédéric Poidevin, Vijith Jacob Poovelil, Adrian M. Price-Whelan, Anna Bárbara de Andrade Queiroz, M. Jordan Raddick, Amy Ray, Sandro Barboza Rembold, Nicole Riddle, Rogemar A. Riffel, Rogério Riffel, Hans-Walter Rix, Annie C. Robin, Aldo Rodríguez-Puebla, Alexandre Roman-Lopes, Carlos Román-Zúñiga, Benjamin Rose, Ashley J. Ross, Graziano Rossi, Kate H. R. Rubin, Mara Salvato, Sebastián F. Sánchez, José R. Sánchez-Gallego, Robyn Sanderson, Felipe Antonio Santana Rojas, Edgar Sarceno, Regina Sarmiento, Conor Sayres, Elizaveta Sazonova, Adam L. Schaefer, Ricardo Schiavon, David J Schlegel, Donald P. Schneider, Mathias Schultheis, Axel Schwope, Aldo Serenelli, Javier Serna, Zhengyi Shao, Griffin Shapiro, Anubhav Sharma, Yue Shen, Matthew Shetrone, Yiping Shu, Joshua D. Simon, M. F. Skrutskie, Rebecca Smethurst, Verne Smith, Jennifer Sobeck, Taylor Spoo, Dani Sprague, David V. Stark, Keivan G. Stassun, Matthias Steinmetz, Dennis Stello, Alexander Stone-Martinez, Thaisa Storchi-Bergmann, Guy S. Stringfellow, Amelia Stutz, Yung-Chau Su, Manuchehr Taghizadeh-Popp, Michael S. Talbot, Jamie Tayar, Eduardo Telles, Johanna Teske, Ani Thakar, Christopher Theissen, Andrew Tkachenko, Daniel Thomas, Rita Tojeiro, Hector Hernandez Toledo, Nicholas W. Troup, Jonathan R. Trump, James Trussler, Jacqueline Turner, Sarah Tuttle, Eduardo Unda-Sanzana, José Antonio Vázquez-Mata, Marica Valentini, Octavio Valenzuela, Jaime Vargas-González, Mariana Vargas-Magaña, Pablo Vera Alfaro, Sandro Villanova, Fiorenzo Vincenzo, David Wake, Jack T. Warfield, Jessica Diane Washington, Benjamin Alan Weaver, Anne-Marie Weijmans, David H. Weinberg, Achim Weiss, Kyle B. Westfall, Vivienne Wild, Matthew C. Wilde, John C. Wilson, Robert F. Wilson, Mikayla Wilson, Julien Wolf, W. M. Wood-Vasey, Renbin 人斌Yan 岳, Olga Zamora, Gail Zasowski, Kai Zhang, Cheng Zhao, Zheng Zheng, Zheng Zheng, and Kai Zhu. The seventeenth data release of the Sloan digital sky surveys: Complete release of manga, mastar, and apogee-2 data. *The Astrophysical Journal Supplement Series*, 259(2):35, March 2022. ISSN 1538-4365. doi: 10.3847/1538-4365/ac4414. URL <http://dx.doi.org/10.3847/1538-4365/ac4414>.

Tobias Buck and Christian Schwarz. Deep Multimodal Representation Learning for Stellar Spectra. *arXiv e-prints*, art. arXiv:2410.16081, October 2024. doi: 10.48550/arXiv.2410.16081.

Sven Buder, Sanjib Sharma, Janez Kos, Anish M Amarsi, Thomas Nordlander, Karin Lind, Sarah L Martell, Martin Asplund, Joss Bland-Hawthorn, Andrew R Casey, Gayandhi M De Silva, Valentina D’Orazi, Ken C Freeman, Michael R Hayden, Geraint F Lewis, Jane Lin, Katharine J Schlesinger, Jeffrey D Simpson, Dennis Stello, Daniel B Zucker, Tomaž Zwitter, Kevin L Beeson, Tobias Buck, Luca Casagrande, Jake T Clark, Klemen Čotar, Gary S Da Costa, Richard de Grijs, Diane Feuillet, Jonathan Horner, Prajwal R Kafle, Shourya Khanna, Chiaki Kobayashi, Fan Liu, Benjamin T Montet, Govind Nandakumar, David M Nataf, Melissa K Ness, Lorenzo Spina, Thor Tepper-García, Yuan-Sen Ting(丁源森), Gregor Traven, Rok Vogrinčič, Robert A Wittenmyer, Rosemary F G Wyse, and Maruša Žerjal. The galah+ survey: Third data release. *Monthly Notices of the Royal Astronomical Society*, 506(1):150–201, May 2021. ISSN 1365-2966. doi: 10.1093/mnras/stab1242. URL <http://dx.doi.org/10.1093/mnras/stab1242>.

Andrew R. Casey, David W. Hogg, Melissa Ness, Hans-Walter Rix, Anna Q Y Ho, and Gerry Gilmore. The Cannon 2: A data-driven model of stellar spectra for detailed chemical abundance analyses. *arXiv e-prints*, art. arXiv:1603.03040, March 2016. doi: 10.48550/arXiv.1603.03040.

Johan Comparat, Claudia Maraston, Daniel Goddard, Violeta Gonzalez-Perez, Jianhui Lian, Sofia Meneses-Goytia, Daniel Thomas, Joel R. Brownstein, Rita Tojeiro, Alexis Finoguenov, Andrea Merloni, Francisco Prada, Mara Salvato, Guangtun B. Zhu, Hu Zou, and Jonathan Brinkmann. Stellar population properties for 2 million galaxies from sdss dr14 and deep2 dr4 from full spectral fitting, 2019. URL <https://arxiv.org/abs/1711.06575>.

DESI Collaboration, M. Abdul-Karim, A. G. Adame, D. Aguado, J. Aguilar, S. Ahlen, S. Alam, G. Aldering, D. M. Alexander, R. Alfarsy, L. Allen, C. Allende Prieto, O. Alves, A. Anand, U. Andrade, E. Armengaud, S. Avila, A. Aviles, H. Awan, S. Bailey, A. Baleato Lizancos, O. Ballester, A. Bault, J. Bautista, S. BenZvi, L. Beraldo e Silva, J. R. Bermejo-Climent, F. Beutler, D. Bianchi, C. Blake, R. Blum, A. S. Bolton, M. Bonici, S. Brieden, A. Brodzeller, D. Brooks, E. Buckley-Geer, E. Burtin, R. Canning, A. Carnero Rosell, A. Carr, P. Carrilho, L. Casas, F. J. Castander, R. Cereskaité, J. L. Cervantes-Cota, E. Chaussidon, J. Chaves-Montero, S. Chen, X. Chen, T. Claybaugh, S. Cole, A. P. Cooper, M. C. Cousinou, A. Cuceu, T. M. Davis, K. S. Dawson, R. de Belsunce, R. de la Cruz, A. de la Macorra, A. de Mattia, N. Deiosso, J. Della Costa, R. Demina, U. Demirbozan, J. DeRose, A. Dey, B. Dey, J. Ding, Z. Ding, P. Doel, K. Douglass, M. Dowicz, H. Ebina, J. Edelstein, D. J. Eisenstein, W. Elbers, N. Emas, S. Escoffier, P. Fagrelius, X. Fan, K. Fanning, V. A. Fawcett, E. Fernández-García, S. Ferraro, N. Findlay, A. Font-Ribera, J. E. Forero-Romero, D. Forero-Sánchez, C. S. Frenk, B. T. Gänsicke, L. Galbany, J. García-Bellido, C. Garcia-Quintero, L. H. Garrison, E. Gaztañaga, H. Gil-Marín, O. Y. Gnedin, S. Gontcho A Gontcho, A. X. Gonzalez-Morales, V. Gonzalez-Perez, C. Gordon, O. Graur, D. Green, D. Gruen, R. Gsponer, C. Guandalin, G. Gutierrez, J. Guy, C. Hahn, J. J. Han, J. Han, S. He, H. K. Herrera-Alcantar, K. Honscheid, J. Hou, C. Howlett, D. Huterer, V. Iršič, M. Ishak, A. Jacques, J. Jimenez, Y. P. Jing, B. Joachimi, S. Joudaki, R. Joyce, E. Jullo, S. Juneau, N. G. Karaçaylı, T. Karim, R. Kehoe, S. Kent, A. Khederlarian, D. Kirkby, T. Kisner, F. S. Kitaura, N. Kizhuprakkat, H. Kong, S. E. Koposov, A. Kremin, A. Krolewski, O. Lahav, Y. Lai, C. Lamman, T. W. Lan, M. Landriau, D. Lang, J. U. Lange, J. Lasker, J. M. Le Goff, L. Le Guillou, A. Leauthaud, M. E. Levi, S. Li, T. S. Li, K. Lodha, M. Lokken, Y. Luo, C. Magneville, M. Manera, C. J. Manser, D. Margala, P. Martini, M. Maus, J. McCullough, P. McDonald, G. E. Medina, L. Medina-Varela, A. Meisner, J. Mena-Fernández, A. Menegas, M. Mezcua, R. Miquel, P. Montero-Camacho, J. Moon, J. Moustakas, A. Muñoz-Gutiérrez, D. Muñoz-Santos, A. D. Myers, J. Myles, S. Nadathur, J. Najita, L. Napolitano, J. A. Newman, F. Nikakhtar, R. Nikutta, G. Niz, H. E. Noriega, N. Padmanabhan, E. Paillas, N. Palanque-Delabrouille, A. Palmese, J. Pan, Z. Pan, D. Parkinson, J. Peacock, W. J. Percival, A. Pérez-Fernández, I. Pérez-Ràfols, P. Peterson, J. Piat, M. M. Pieri, M. Pinon, C. Poppett, A. Porredon, F. Prada, R. Pucha, F. Qin, D. Rabinowitz, A. Raichoor, C. Ramírez-Pérez, S. Ramirez-Solano, M. Rashkovetskyi, C. Ravoux, A. H. Riley, A. Rocher, C. Rockosi, J. Rohlf, A. J. Ross, G. Rossi, R. Ruggeri, V. Ruhlmann-Kleider, C. G. Sabiu, K. Said, A. Singtone, L. Samushia, E. Sanchez, N. Sanders, C. Saulder, E. F. Schlaflly, D. Schlegel, D. Scholte, M. Schubnell, H. Seo, A. Shafieloo, R. Sharples, J. Silber, M. Siudek, A. Smith, D. Sprayberry, J. Suárez-Pérez, J. Swanson, T. Tan, G. Tarlé, P. Taylor, G. Thomas, R. Tojeiro, R. J. Turner, W. Turner, L. A. Ureña-López, R. Vaisakh, M. Valluri, M. Vargas-Magaña, L. Verde, M. Walther,

B. Wang, M. S. Wang, W. Wang, B. A. Weaver, N. Weaverdyck, R. H. Wechsler, M. White, M. Wolfson, J. Yang, C. Yèche, S. Youles, J. Yu, S. Yuan, E. A. Zaborowski, P. Zarrouk, H. Zhang, C. Zhao, R. Zhao, Z. Zheng, R. Zhou, H. Zou, S. Zou, and Y. Zu. Data release 1 of the dark energy spectroscopic instrument, 2025. URL <https://arxiv.org/abs/2503.14745>.

Alexey Dosovitskiy, Lucas Beyer, Alexander Kolesnikov, Dirk Weissenborn, Xiaohua Zhai, Thomas Unterthiner, Mostafa Dehghani, Matthias Minderer, Georg Heigold, Sylvain Gelly, Jakob Uszkoreit, and Neil Houlsby. An Image is Worth 16x16 Words: Transformers for Image Recognition at Scale, June 2021. URL <http://arxiv.org/abs/2010.11929>.

Ana E. García Pérez, Carlos Allende Prieto, Jon A. Holtzman, Matthew Shetrone, Szabolcs Mészáros, Dmitry Bizyaev, Ricardo Carrera, Katia Cunha, D. A. García-Hernández, Jennifer A. Johnson, Steven R. Majewski, David L. Nidever, Ricardo P. Schiavon, Neville Shane, Verne V. Smith, Jennifer Sobeck, Nicholas Troup, Olga Zamora, David H. Weinberg, Jo Bovy, Daniel J. Eisenstein, Diane Feuillet, Peter M. Frinchaboy, Michael R. Hayden, Fred R. Hearty, Duy C. Nguyen, Robert W. O’Connell, Marc H. Pinsonneault, John C. Wilson, and Gail Zasowski. Aspcap: The Apogee Stellar Parameter and Chemical Abundances Pipeline. *The Astronomical Journal*, 151(6):144, 2016. ISSN 1538-3881. doi: 10.3847/0004-6256/151/6/144. URL <http://dx.doi.org/10.3847/0004-6256/151/6/144>.

Nolan Koblischke and Jo Bovy. Spectrafm: Tuning into stellar foundation models, 2024. URL <https://arxiv.org/abs/2411.04750>.

Henry W Leung and Jo Bovy. Deep learning of multi-element abundances from high-resolution spectroscopic data. *Monthly Notices of the Royal Astronomical Society*, November 2018. ISSN 0035-8711, 1365-2966. doi: 10.1093/mnras/sty3217. URL <https://academic.oup.com/mnras/advance-article/doi/10.1093/mnras/sty3217/5212314>.

Ilya Loshchilov and Frank Hutter. Decoupled weight decay regularization, 2019. URL <https://arxiv.org/abs/1711.05101>.

Peter Melchior, Yan Liang, ChangHoon Hahn, and Andy Goulding. Autoencoding Galaxy Spectra I: Architecture, November 2022. URL <http://arxiv.org/abs/2211.07890>.

Richard Olney, Marina Kounkel, Chad Schillinger, Matthew T. Scoggins, Yichuan Yin, Erin Howard, K. R. Covey, Brian Hutchinson, and Keivan G. Stassun. Apogee net: Improving the derived spectral parameters for young stars through deep learning. *The Astronomical Journal*, 159(4):182, April 2020. ISSN 1538-3881. doi: 10.3847/1538-3881/ab7a97. URL <http://dx.doi.org/10.3847/1538-3881/ab7a97>.

Liam Parker, Francois Lanusse, Siavash Golkar, Leopoldo Sarra, Miles Cranmer, Alberto Bietti, Michael Eickenberg, Geraud Krämer, Michael McCabe, Rudy Morel, Ruben Ohana, Mariel Petree, Bruno Régaldo-Saint Blanchard, Kyunghyun Cho, and Shirley Ho. Astroclip: a cross-modal foundation model for galaxies. *Monthly Notices of the Royal Astronomical Society*, 531(4):4990–5011, June 2024. ISSN 1365-2966. doi: 10.1093/mnras/stae1450. URL <http://dx.doi.org/10.1093/mnras/stae1450>.

Stephen K.N. Portillo, John K. Parejko, Jorge R. Vergara, and Andrew J. Connolly. Dimensionality reduction of SDSS spectra with variational autoencoders. *arXiv*, 2020. ISSN 23318422. doi: 10.3847/1538-3881/ab9644.

Ph. Prugniel and C. Soubiran. A database of high and medium-resolution stellar spectra. *Astronomy & Astrophysics*, 369(3):1048–1057, April 2001. ISSN 1432-0746. doi: 10.1051/0004-6361:20010163. URL <http://dx.doi.org/10.1051/0004-6361:20010163>.

Maria Rizhko and Joshua S. Bloom. AstroM\$^3\$: A self-supervised multimodal model for astronomy, November 2024. URL <http://arxiv.org/abs/2411.08842>.

Tomasz Różański, Yuan-Sen Ting, and Maja Jabłońska. Toward a Spectral Foundation Model: An Attention-Based Approach with Domain-Inspired Fine-Tuning and Wavelength Parameterization, June 2023. URL <http://arxiv.org/abs/2306.15703>.

Michael J. Smith, Ryan J. Roberts, Eirini Angeloudi, and Marc Huertas-Company. AstroPT: Scaling Large Observation Models for Astronomy. *arXiv e-prints*, art. arXiv:2405.14930, May 2024. doi: 10.48550/arXiv.2405.14930.

The Multimodal Universe Collaboration, Jeroen Audenaert, Micah Bowles, Benjamin M. Boyd, David Chemaly, Brian Cherinka, Ioana Ciucă, Miles Cranmer, Aaron Do, Matthew Grayling, Erin E. Hayes, Tom Hehir, Shirley Ho, Marc Huertas-Company, Kartheik G. Iyer, Maja Jablonska, Francois Lanusse, Henry W. Leung, Kaisey Mandel, Juan Rafael Martínez-Galarza, Peter Melchior, Lucas Meyer, Liam H. Parker, Helen Qu, Jeff Shen, Michael J. Smith, Connor Stone, Mike Walmsley, and John F. Wu. The multimodal universe: Enabling large-scale machine learning with 100tb of astronomical scientific data, 2024. URL <https://arxiv.org/abs/2412.02527>.

Ashish Vaswani, Noam Shazeer, Niki Parmar, Jakob Uszkoreit, Llion Jones, Aidan N. Gomez, Lukasz Kaiser, and Illia Polosukhin. Attention Is All You Need, 2017. URL <http://arxiv.org/abs/1706.03762>.

Xiaosheng Zhao, Yang Huang, Guirong Xue, Xiao Kong, Jifeng Liu, Xiaoyu Tang, Timothy C. Beers, Yuan-Sen Ting, and A-Li Luo. SpecCLIP: Aligning and Translating Spectroscopic Measurements for Stars. *arXiv e-prints*, art. arXiv:2507.01939, July 2025. doi: 10.48550/arXiv.2507.01939.

Fucheng Zhong, Nicola R. Napolitano, Caroline Heneka, Rui Li, Franz Erik Bauer, Nicolas Bouche, Johan Comparat, Young-Lo Kim, Jens-Kristian Krogager, Marcella Longhetti, Jonathan Loveday, Boudewijn F. Roukema, Benedict L. Rouse, Mara Salvato, Crescenzo Tortora, Roberto J. Assef, Letizia P. Cassarà, Luca Costantin, Scott M. Croom, Luke J. M. Davies, Alexander Fritz, Guillaume Guiglion, Andrew Humphrey, Emanuela Pompei, Claudio Ricci, Cristóbal Sifón, Elmo Tempel, and Tayyaba Zafar. Galaxy Spectra neural Network (GaSNet). II. Using deep learning for spectral classification and redshift predictions. *Monthly Notices of the Royal Astronomical Society*, 532(1): 643–665, July 2024. doi: 10.1093/mnras/stae1461.